

# Numerical simulations of heat transport in photothermal measurement techniques

X. FILIP<sup>a\*</sup>, M. CHIRTOC<sup>b</sup>, J. PELZL<sup>c</sup>

<sup>a</sup>National R&D Institute for Isotopic and Molecular Technologies, P.O.Box 700, 400293, Cluj-Napoca 5, Romania

<sup>b</sup>LTP, UTAP, Université de Reims, BP 1039, 51687 Reims Cedex 2, France

<sup>c</sup>Inst. für Experimentalphysik III, Festkörperspektroskopie, Ruhr-Universität, 44801 Bochum, Germany

Thermal parameters of a sample can be determined using photothermal measurement techniques and a theoretical model of modulated heat transport. This model is represented by a partial differential equation having a set of corresponding boundary and initial conditions. Unfortunately, it is not always possible to obtain the analytical solutions (useful to interpret the experimental results) and in this case, the solutions are obtained by numerical methods. We used a software based on the finite element method to analyze the heat conduction in such cases. The versatility of the method is shown by some examples illustrating the 1D and 3D heat conduction. A comparison with experimental results is presented.

(Received December 2, 2005; accepted May 18, 2006)

**Keywords:** Photothermal techniques, Numerical simulations, Finite element method

## 1. Introduction

When incident light is absorbed by a material, the resulting heat generation leads to so called photothermal (PT) phenomena. Along with the increasing possibilities of laser light generation, PT phenomena have been investigated and exploited more and more for material characterization. Photothermal techniques have been established for many years as a tool for non-destructive evaluation of material properties [1]. Briefly, the common working principle of conventional photothermal techniques is based on the study of the periodic temperature distribution, i.e., the thermal wave, produced in a given sample as a result of heating due to an intensity modulated pump laser source impinging on the surface. Thermal waves inside a homogeneous sample diffuse over a characteristic distance, which is given by the thermal diffusion length (it depends on the thermal diffusivity  $\alpha$  and the modulation frequency  $f$ ,  $\mu = (\alpha/\pi f)^{1/2}$ ) [2]. During the last few years, photothermal techniques have been used in a wide variety of fields including material science [3-5], agriculture [6], medical and environmental sciences [7].

The continuous reduction of the size of semiconductor devices is associated with an increase of the dissipated power densities. Therefore thermal aspects have received increasing attention in the semiconductor technology. To detect and to control local heat dissipation or local thermal defects, which could lead to overheating effects, experimental techniques for monitoring temperature and thermal properties with a high spatial resolution are required. Such techniques are scanning thermal microscopy – SThM, and scanning thermal expansion microscopy – SThEM, for measuring the thermal structure at micro- and nanoscale [8,9].

To extract from experimental data the unknown thermal properties of the investigated sample, the normalized measured values (phase and amplitude) are correlated with the results of theoretical approximations. From theoretical point of view, the problem of modulated

heat conduction is a mathematical model of a physical situation. This model is represented by a partial differential equation having a set of corresponding boundary and initial conditions. The analytical solution of this equation has two parts: a homogeneous part (provides information regarding the natural behavior of the system: thermal conductivity, diffusivity, etc.) and a particular part (describes the disturbance in the system: heat generation, temperature difference in a medium, etc.). This solution can be obtained only in some particular cases: simple geometry of the sample and in general the case of 1D heat conduction [10] specific to high modulation frequency. At low modulation frequency it must be considered the gaussian form of the laser beam and the fact that heat propagation has a 3D dimension. In this case and for complex systems, the heat conduction equation can be solved only by numerical methods.

There are two common classes of numerical methods used to solve such problems: finite difference method [11] and finite element method [12]. The advantage of finite difference method is that it is easy to understand and employ in simple problems, but it is difficult to apply to problems with complex boundary conditions (or for nonisotropic material properties). Due to the complexity of the thermal investigation techniques applied to analyze the heat dissipation in complex systems (like microelectronic devices) we propose the finite element method to investigate the harmonic heat transport.

## 2. Theoretical model

In photothermal radiometric (PTR) measurements (Fig. 1) the sample is irradiated with a modulated gaussian laser beam and the infrared radiation (amplitude and phase) emitted by the heated sample surface is being measured.

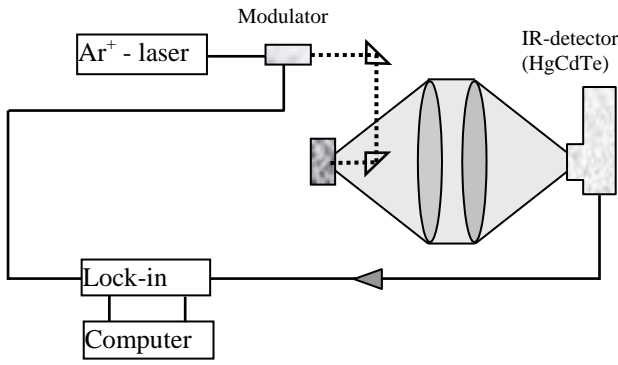


Fig. 1. Experimental set-up for PTR measurements.

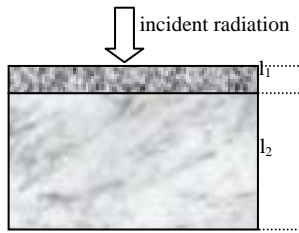


Fig. 2. Two-layer sample.

The basic equation of heat conduction in an isotropic body with temperature dependent heat transfer is [13]:

$$-\left(\frac{\partial q_x}{\partial x} + \frac{\partial q_y}{\partial y} + \frac{\partial q_z}{\partial z}\right) + Q(x, y, z, t) = \rho c \frac{\partial T}{\partial t} \quad (1)$$

where  $q_x$ ,  $q_y$ ,  $q_z$  are components of heat flux,  $Q(x, y, z, t)$  is the inner heat generation rate per unit volume,  $\rho$  - material density,  $c$  - heat capacity. According to Fourier's law:

$$q_x = -k \frac{\partial T}{\partial x} ; \quad q_y = -k \frac{\partial T}{\partial y} ; \quad q_z = -k \frac{\partial T}{\partial z} \quad (2)$$

with  $k$  - thermal conductivity, we obtain:

$$\frac{\partial}{\partial x} \left( k \frac{\partial T}{\partial x} \right) + \frac{\partial}{\partial y} \left( k \frac{\partial T}{\partial y} \right) + \frac{\partial}{\partial z} \left( k \frac{\partial T}{\partial z} \right) + Q(x, y, z, t) = \rho c \frac{\partial T}{\partial t} \quad (3)$$

having: a) boundary conditions: specified temperature at the surface, specified heat flow on a surface, convection, radiation; b) initial conditions (for transient problem); c) continuity conditions of temperature and heat flux at the interface between different materials [10].

The expression of heat generation is given by:

a) 1D case [14]:

$$Q(z, t) = -\eta \frac{dI(z, t)}{dz} = \eta \beta \frac{I_0}{2} e^{-\beta z} \text{Re}(1 + e^{i\omega t}) \quad (4)$$

where  $\beta$  is the optical absorption constant of the surface layer,  $\eta$  is the ratio of the intensity of the unreflected part of the radiation to the total incident intensity,  $I_0$  is the amplitude of the incident radiation and  $\omega$  is related to the modulation frequency  $f$  of the intensity by  $\omega = 2\pi f$ .

b) 3D case (axial symmetry - Henkel transformation) [15]:

$$Q(r, z, t) = \eta \beta \frac{2I_0}{\pi r_H^2} e^{-2r^2/r_H^2} e^{-\beta z} \text{Re}(1 + e^{i\omega t}) \quad (5)$$

The partial differential equation (Eq. 3) can be solved by considering the solution having two components, a stationary and a time-dependent one [15]. For the two-layer sample in Fig. 2 (highly opaque and semi-infinite approximation for  $l_2$ ) the time dependent solution, at the surface, is:

a) in 1D heat conduction model, valid at high modulation frequency:

$$\delta T_s(f, t) = \frac{\eta I_0}{2k_1 \sigma_1} \cdot \frac{1 + R_{12} e^{-2\sigma_1 l_1}}{1 - R_{12} e^{-2\sigma_1 l_1}} e^{i(2\pi f t - \pi/4)} \quad (6)$$

$$\sigma_1 = (i+1) \sqrt{\frac{\pi f}{\alpha_1}} ;$$

$$R_{12} = \frac{k_1 \sigma_1 - k_2 \sigma_2}{k_1 \sigma_1 + k_2 \sigma_2} \quad (7)$$

$R_{12}$  is the thermal reflection coefficient between the surface layer and the substrate, and is given by  $R_{12} = (g_{12} - 1)/(g_{12} + 1)$ . The ratio  $g_{12} = e_1/e_2$  represents the ratio of thermal effusivities and  $\alpha_i$  ( $i = 1, 2$ ) is the thermal diffusivity.

b) in 3D heat conduction model, valid at low frequency and considering cylindrical symmetry

$$\delta T_s^H(\lambda, z=0, f, t) = \frac{\eta I_0 e^{-\lambda^2 r_H^2/8}}{2\pi k_1 \lambda_1} \left[ \frac{1 + R_{12}(\lambda, f) e^{-2\lambda_1(\lambda, f) l_1}}{1 - R_{12}(\lambda, f) e^{-2\lambda_1(\lambda, f) l_1}} \right] e^{i2\pi f t} \quad (8)$$

where  $\delta T_s^H$  represents the Henkel transform surface temperature,  $\lambda_1(\lambda, f) = \text{sqrt}(\lambda^2 + \sigma_1^2(f))$  and  $\lambda$  is the Henkel parameter.  $r_H$  is the radius at which the Gaussian distribution of laser beam dropped to  $1/e^2$  of its peak value. The complex surface temperature can be calculated by a inverse Henkel transform [15].

In both 1D and 3D cases, the analytical solution can be obtained only for simple systems (in this case a two-layer model with uniform layer thickness). For samples with complicated geometries are necessary numerical simulations.

### 3. Results and discussion

To simulate the heat conduction we used the ANSYS software, based on finite element (FE) method. The FE method is a numerical technique for solving problems which are described by partial differential equations or can be formulated as functional minimization [16]. The domain of interest is represented as an assembly of finite elements connected by nodes. The results are nodal values of a physical field, which is sought. That means that a continuous physical problem is transformed into discretized finite element problem with unknown nodal values. Values inside finite elements can be recovered using these nodal values. The ANSYS software, based on this method, can do many types of simulations from thermal analysis, structural analysis, electromagnetic and so on.

Briefly, the software is organized in two levels: the Begin level and the Processor level (Fig. 3). A typical analysis in ANSYS involves three distinct steps. In preprocessing step, using the Prep7 processor we provide

to the software the data, such as: geometry and material properties of the sample, and we choose the element type. In the *solution step*, using the Solution processor we define the type of analysis, set boundary conditions, apply loads and initiate finite element solution. In *postprocessing step*,

using Post1 (for static or steady state problems) or Post26 (for transient problems) we can review the results of the analysis through graphical display and tabular listings [16].

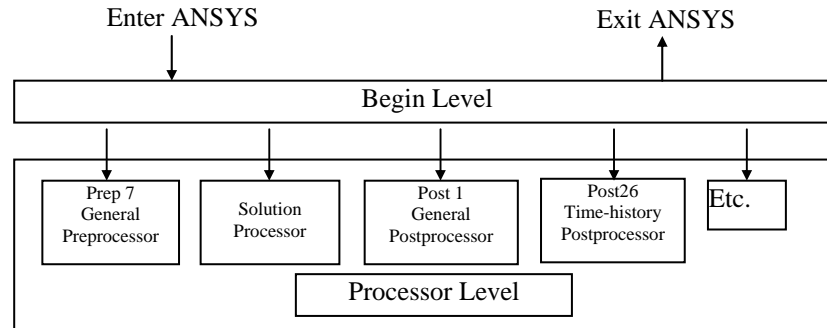


Fig. 3. ANSYS software organization.

The main sources of errors that can contribute to incorrect results are:

i) *Wrong input data, such as physical properties and dimensions.* Listing and verifying physical properties and coordinates of nodes and keypoints before proceeding any further with the analysis can simply correct this kind of errors.

ii) *Selecting inappropriate types of elements.* This can be corrected only by understanding the underlying theory of the FE method and of the process, which will be modeled.

iii) *Poor element shape and size after meshing.* The meshing is a very important part of the FE analysis. Inappropriate element shape and size will influence the accuracy of the results.

iv) *Applying wrong boundary conditions and loads.* This is the most difficult aspect of modeling and requires good judgment and some experience.

Before we use this software to interpret some experimental data we have to test its limits by comparison with an analytical solution. For this purpose we consider a simple case of 1D heat conduction: a two-layer sample (a thin surface layer deposited on a substrate, see Fig. 2) uniformly heated at the surface. The analytical solution at the surface has the expression given by Eq. (6). It is a complex expression characterized by amplitude and phase. This expression was obtained considering a semi-infinite approximation for the substrate. In Fig. 4 there are represented the analytical and numerical results for this case.

The numerical results were obtained in different conditions (different meshing and substrate thicknesses). We can observe, especially from phase dependency, that in some frequency ranges, the numerical results are different from analytical solution:

a) at low frequency, for too thin substrate even with high meshing;

b) at high frequency for low meshing.

That means that for those frequencies the element size was too big or the thickness of the substrate was too small. Because in ANSYS there is a limited number of nodes and elements that can be used, the questions are: (i) how small should be the elements, and (ii) how thick should be the

substrate in order to obtain good results. The best solution is the one that uses the simplest model but which still approximates well the physical situation.

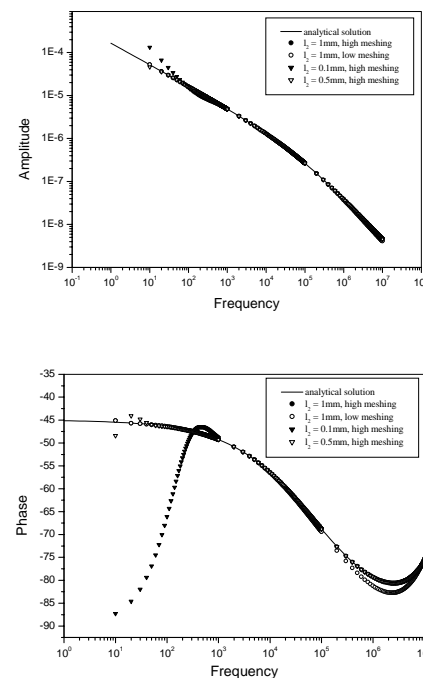


Fig. 4. Comparison between analytical solution and numerical simulation (amplitude and phase - 1D case) of heat transport in a two-layer sample.

To answer these questions we made some test simulations. First, we simulate the modulated heat transport in a bulk sample (sigradur, having a semi-infinite thickness from photothermal point of view) with a uniform heat flux at the surface (that means 1D case) for different meshing (different element size). We made these simulations at 10 Hz and considering the thermal properties of sigradur:  $\rho = 1420 \text{ kg/m}^3$ ,  $c = 824 \text{ J/kg}\cdot\text{K}$ ,  $k = 4.92 \text{ W/m}\cdot\text{K}$ .

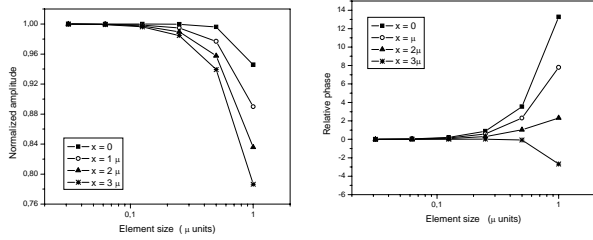


Fig. 5. Normalized amplitude and relative phase versus element size for different depths from the surface of the sample ( $x = 0, 1\mu, 2\mu, 3\mu$ ;  $\mu$  is the thermal diffusion length at 10 Hz).

At this frequency the thermal diffusion length for sigradur is  $\mu = 3.65 \times 10^{-4}$  m. The thickness of the sample was  $d = 6 \cdot \mu = 21.9 \times 10^{-4}$  m. We compared the results (amplitude and phase) obtained at different depths in the sample for different element size (Fig. 5). For a better comparison we represented the normalized amplitude (at the value corresponding to smallest element size) and relative phase in function of element size (in thermal lengths units). The mesh refinement is optimal when there are no or little changes in the solution. From Fig. 5 it can be seen that for an element size smaller than  $\mu/10$  the errors are very small. In a simple thermal wave problem where the frequency-dependent amplitude and frequency-dependent phase of the surface temperature are of interest, the model must be non-uniformly meshed from the top to the bottom of the sample with more mesh refinement beneath the sample surface. On the other hand, when we are interested to measure the thermal expansion of a sample, we must be care, also, at the element size in depths of the sample. And that is the reason for we made simulations at different depths in the sample.

To answer the question about the thickness of the substrate we made some test simulations, at 10Hz, with an element size of  $\mu/10$  and we compared the results obtained at different depths in the sample (Fig. 6).

From Fig. 6 we can conclude that for a thickness of about  $2.5 - 3 \mu$ , the sample can be considered as semi-infinite (from phothermal point of view). That means that for a real case we have to consider distances of about  $3 \mu$  around the heat spot. This fact will increase the speed of simulation by minimizing the numbers of nodes involved in the differential equations and it allows avoiding the computation of too much data which are useless.

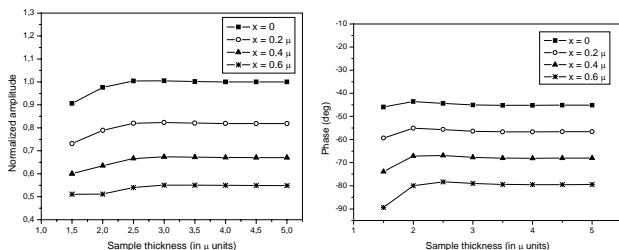


Fig. 6. Dependence by sample thickness of normalized amplitude and phase, at different depths in the sample ( $x = 0, 0.2, 0.4, 0.6 \mu$ ).

Considering these facts we simulate 3D heat conduction in a two-layer system. Good agreement with the analytical solution is obtained by adapting the geometry and the element size with the frequency.

The last test of the software was a comparison with experimental data. Another photothermal technique used to investigate the thermal properties of the sample is the photopyroelectric technique. This detection method consists of measuring the temperature increase of a sample (excited by a modulated laser beam), by placing a pyroelectric transducer (sensor) in thermal contact with the sample [18]. If the sensor is placed at the rear face of the sample where excitation takes place, then the configuration is said inverse (front). Otherwise, the configuration is said standard (back).

Using the front configuration we measured the thermal properties of an adhesive tape. On a side of a Cu bar of dimensions  $60 \times 10.5 \times 12.5 \text{ mm}^3$ , we put an adhesive tape and a pyroelectric sensor (the adhesive tape make the contact between the sensor and the Cu bar) having the dimensions of  $6.18 \times 6.18 \text{ mm}^3$ .

The thickness of the adhesive tape was 0.092 mm, and of the sensor 0.255 mm (Fig. 7). The pyroelectric sensor was irradiated with a modulated laser beam, having the radius of 1.5 mm. Because the system does not have an axial symmetry, we have to use a 3D modeling. We modeled a quarter of the sample and we made a uniform meshing in sensor and adhesive tape to have control on applying loads and read results (Fig. 8). In Cu bar we choose an automatic mesh, refined at the interface with the sample.

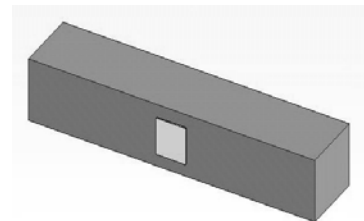


Fig. 7. Geometry of the sample.

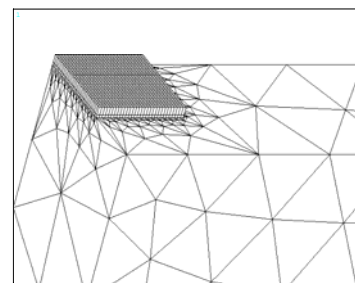


Fig. 8. The meshing used in ANSYS simulations for a quarter of the sample in Fig. 7.

The comparison of numerical results with the experimental data are presented in Fig. 9, for amplitude and phase.

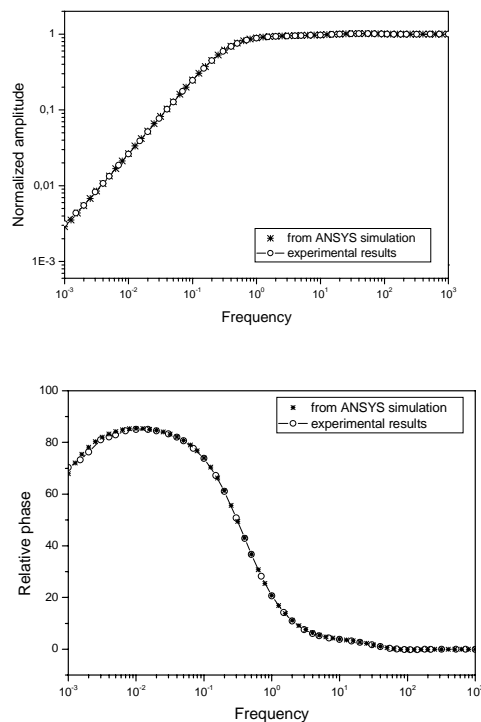


Fig. 9. Comparison between numerical simulation and experimental data in a direct PPE experiment.

As it can be seen from Fig. 9, a very good agreement between numerical and experimental results was obtained.

## 5. Conclusions

In contrast to analytical solutions, which show the exact behaviour of a system at any point within the system, numerical solutions approximate exact solutions only at discrete points, called nodes. Despite this fact, if during the simulation we take into account all the theoretical and experimental aspects, we can obtain very good agreements between the numerical and experimental results. The main goal of this work was to test the limits and to demonstrate the versatility of ANSYS software in simulating modulated heat transfer in photothermal techniques. Our results demonstrate that this software, based on FE method, can be applied with success to investigate the heat transport in samples with complicated geometry.

The advantages of FE method are: *i*) can handle complex geometry (the heart and power of the finite element method), *ii*) can handle complex analysis type (vibration, transients, nonlinear, heat transfer, fluids), *iii*) can handle complex loading (nodal, surface or volum loads, time or frequency dependent loads).

The disadvantages are: *i*) a powerful computer and reliable FEM software are essential; *ii*) input and output data may be large and tedious to prepare and interpret; *iii*) susceptibility to user-introduced modeling errors (poor choice of elements type, distorted elements, geometry not adequately modeled).

## Acknowledgements

Dr. Xenia Filip and Dr. Mihai Chirtoc are grateful for the support of "Al. von Humboldt" Foundation, Germany, for carrying out this work.

## References

- [1] G. Busse, H. G. Walther, in Progress in Photothermal And Photoacoustic Science and Technology, Vol. I: Principles and Perspectives of Photothermal and Photoacoustic Phenomena, Chap. 5, pp. 207-298, edited by A. Mandelis, Elsevier, New York (1992).
- [2] A. Mandelis, S. Paolini, L. Nicolaides, Rev. of Sci. Instruments, **71**(6), 2440 (2000).
- [3] J. E. de Albuquerque, W. L. B. Melo, R. M. Faria, Rev. of Sci. Instruments, **74**(1), 306 (2003).
- [4] C. Christofides, Critical rev. in Sol. State and Materials science, **18**(2), 113 (1993).
- [5] A. Mandelis, C.H. Wang, Ferroelectrics **236**, 235 (2000).
- [6] D. Bicanic (Ed), Food Characterization and analysis by photoacoustic and photothermal methods, Final Report IC 15CT 961003, European Commission DG XII R&D Brussels (1999).
- [7] A. Mandelis, P. Hess (Eds), Medical, Environmental, Biological and Agricultural Sciences, in "Progress in Photothermal and Photoacoustic Sciences and Technology", PTR Prentice Hall, Englewood Cliffs, New Jersey (1998).
- [8] J. Pelzl, J. Bolte, F. Niebsch, D. Dietzel, H. H. Althaus, Analytical Science, **17**, s53 (2001).
- [9] D. Dietzel, J. Gibkes, S. Chotikaprakhan, B.K. Bein, J. Pelzl, Int. J. of Thermophysics, **24**(3), 741 (2003).
- [10] H. S. Carslaw & J.C. Jaeger, Conduction of heat in solids, Oxford University Press (1956).
- [11] J. W. Thomas, Numerical Partial Differential Equations: Finite Difference Methods, Springer-Verlag, New-York (1995).
- [12] K. H. Huebner, D. L. Dewhirst, D. E. Smith, T. G. Byron, John Wiley & Sons, New York (2001).
- [13] D. Almond, P. Patel, Photothermal Science and Techniques, Chapman & Hall, London, UK (1996).
- [14] B. K. Bein, J. Pelzl, Analysis of Surfaces Exposed to Plasmas by Nondestructive Photoacoustic and Photothermal Techniques, in PLASMA DIAGNOSTICS, vol.2, Surface Analysis and Interactions (eds. O. Auciello, D.L. Flamm), Academic Press (1989).
- [15] J. L. Fotsing, Investigation of Thermal Transport in Layered Systems and Micro-structured Semiconductor Devices by Photothermal Techniques and Finite Element Simulations, Diploma Thesis, Ruhr Universität Bochum, Germany (2004).
- [16] Saeed Moaveni, Finite Element Analysis: Theory and Applications with ANSYS, Prentice Hall, 2<sup>nd</sup> edition (2003).
- [17] D. Dietzel, S. Chotikaprakhan, X. Filip, M. Chirtoc, H. Bangert, C. Eisenmenger-Sittner, E. Neubauer, J. Pelzl, B. K. Bein, 14<sup>th</sup> Int. Colloquium on plasma Processes, CIP 2003, Antibes, France, Ed. SVF, Paris, 2003, p 264 .
- [18] M. Chirtoc, G. Mihailescu, Phys. Rev. **B 40**, 906 (1989).

\*Corresponding author: xenia\_filip@yahoo.com